Talanta 86 (2011) 133–141

Contents lists available at SciVerse ScienceDirect

Talanta

journal homepage: www.elsevier.com/locate/talanta

Glucose detection with surface plasmon resonance spectroscopy and molecularly imprinted hydrogel coatings

Jing Wang[a], Soame Banerji[b], Nicola Menegazzo[a], Wei Peng[b,1], Qiongjing Zou[a], Karl S. Booksh[a,*]

[a] Department of Chemistry and Biochemistry, University of Delaware, Newark, DE 19711, United States
[b] Department of Chemistry and Biochemistry, Arizona State University, Tempe, AZ, 85287, United States

ARTICLE INFO

Article history:
Received 12 July 2011
Received in revised form 22 August 2011
Accepted 23 August 2011
Available online 30 August 2011

Keywords:
Surface plasmon resonance
Molecular imprinting
Hydrogel
Gold nanoparticles
Glucose sensing

ABSTRACT

Molecularly imprinted hydrogel membranes were developed and evaluated for detection of small analytes via surface plasmon resonance spectroscopy. Imprinting of glucose phosphate barium salt into a poly(allylamine hydrochloride) network covalently bound to gold surfaces yielded a selective sensor for glucose. Optimization of relative amounts of chemicals used for preparation of the hydrogel was performed to obtain highest sensitivity. Addition of gold nanoparticles into the hydrogel matrix significantly amplified its response and sensitivity due to the impact of gold nanoparticles on the refractive index of the sensing layer. Evaluation of its selectivity showed that the sensor displayed preferential recognition to glucose compared to structurally related sugars in addition to being unaffected by phosphate as well as compounds containing amine groups, like creatinine. The detection limit of glucose in deionized water was calculated to be 0.02 mg/mL. The developed sensor was finally exposed to human urine spiked with glucose illustrating the coating's ability to re-bind the analyte in complex matrices. While the working concentration range in water was determined to be suitable for glucose monitoring in diabetic individuals at physiological levels, the detection in urine was determined to be 0.12 mg/mL. The decreased performance in urine provided an initial perspective on the difficulties associated with measurements in complex media.

1. Introduction

Monitoring of small molecules, such as metabolites, drugs, pesticides, and pollutants in complex matrices is of interest to environmental analysis, medical studies, clinical treatment and food science [1–7]. Surface plasmon resonance (SPR) spectroscopy is a versatile approach capable of detecting a wide range of small molecules upon incorporation of appropriate surface modification strategies [8–13]. In the Kretschmann configuration, surface plasmon polaritons (SPPs) are excited by backside-illuminating the plasmon supporting material (typically gold or silver) via total internal reflectance [14–16]. SPR spectroscopic sensing measures changes in the dielectric constant (ultimately, the refractive index, RI) of the sample induced by either chemical (e.g. antibody–antigen binding) or physical (e.g. temperature) events. The analytical signal is derived from the intensity minima of the reflected light (the so-called 'SPR dip') which corresponds to photons momentum matched to SPPs, and is measured as a function of in-coupling angle (for monochromatic light sources) or wavelength (for fixed-angle configurations). SPR spectroscopy displays high sensitivity towards biomolecular binding events, as evidenced by low detection limits reported (ng/mL level [15,17]), as well as capability for real-time monitoring, rendering it an important tool in (bio)chemical analyses [15,16,18,19].

However, RI measurements are not inherently selective, therefore non-specific events originating from interferents present a challenge to SPR sensors. To overcome this limitation, different analyte recognition strategies have been incorporated [20]. Molecularly imprinted polymers (MIPs) and molecularly imprinted hydrogels (MIHs) consist of biomimetic matrices templated with a target analyte, yielding recognition sites capable of selectively re-binding the analyte [21]. Imprinted matrices have been regarded as an attractive approach towards improvement of sensor selectivity [22–25], due to their versatility, chemical robustness, simple preparation and extended shelf-life compared to biosensing strategies (e.g., enzymes, antibodies). However, adoption of imprinted coatings for SPR sensing has been limited despite initial positive reports from the literature [9,26–28].

Glucose detection is important for health monitoring in diabetic individuals [29,30]. Furthermore, accurate quantification of glucose in untreated physiological fluids, such as urine, remains challenging due to the complexity of the background matrix. Several examples

* Corresponding author. Tel.: +1 302 831 2625; fax: +1 302 831 6335.
E-mail address: kbooksh@udel.edu (K.S. Booksh).
[1] Current address: College of Physics and Optoelectronics Engineering, Dalian University of Technology, Dalian, 116024, China.

0039-9140/$ – see front matter © 2011 Elsevier B.V. All rights reserved.
doi:10.1016/j.talanta.2011.08.046

of commercial glucose sensors are available; however, limitations on the long-term storage, resulting from degradation of the enzymes used for molecular recognition, has fueled investigations in alternative sensing strategies [31], with biomimetic materials, like MIPs, becoming a focus [24,32–34]. Hydrogels consist of a class of hydrophilic polymers capable of absorbing a high fraction of water [35,36], therefore diffusion, and ultimately detection, of polar glucose molecules through these hydrophilic membranes is facilitated. The coatings developed in this work consist of crosslinked poly(allylamine hydrochloride) (PAH) templated with the D-glucose 6-phosphate monobarium salt (GPS-Ba), the hydrogel is then covalently bound to gold-coated glass slides to produce the chemical recognition sites. In addition to health monitoring, the use of glucose as the target analyte also provided a solid baseline to compare the performance of the strategy proposed to other sensing architectures available in the literature and in the market [37].

Binding site formation in molecular imprinting is largely driven by complexation of the template and monomers in solution via hydrogen bonding and π–π stacking [38–40]. Imprinting in solvents that disrupt hydrogen bonding interactions present an additional challenge which can be partially mitigated by employing a template baring a charge. Herein, self-assembly of the positively charged polymer around the template is facilitated by the negatively charged phosphate group. Once the template is removed, detection of glucose (pure, not the barium salt) is achieved following RI changes resulting from physical swelling of the MIH upon binding of the analyte. This sensing platform can be prepared easily, used repeatedly and displays good sensitivity and selectivity towards concentrations lower than 5 mg/mL glucose in aqueous media.

In contrast to detection of biomolecules, SPR sensing of small molecules remains largely unexplored due to the low RI changes induced by the analyte [14], ultimately translating into sensors with comparatively poor sensitivity requiring incorporation of a signal amplification method to improve limits of detection [41–43]. One approach used to improve sensor performance relies on incorporating gold nanoparticles into the chemical recognition matrix [44,45]. In this case, the enhancement phenomenon can be attributed to either an increase in bulk RI due to the presence of nanoparticles and/or plasmonic coupling between the nanoparticles and the underlying continuous metal film [45–51]. Addition of nanoparticles to the MIH amplified the response of the sensor to glucose in water approximately 10-fold. The detection limit, sensitivity and selectivity of the sensor over sugars structurally similar to glucose suggests the ability to measure the analyte at physiologically relevant levels, as well as the prospect of applying similar detection strategies to other low molecular weight compounds.

2. Experimental methods

2.1. Instrumental configuration

Slides used were made from either SF-10 (n = 1.73) or BK-7 (n = 1.52) glass and were coated with 5 nm chromium as an adhesion layer followed by 50 nm of gold by a Cressington 308R DC magnetron sputter coating system (Watford, UK). The SPR system was configured to use the Kretschmann arrangement where the sensor was back-side illuminated with a 5 W Luxeon V white light LED (Lumileds Lighting, LLC, San Jose, CA) through a 60° equilateral prism of the same material as the slide, and the reflected light was transmitted via a linear array of optical fibers to a Jobin-Yvon SPEX 270M spectrometer (Horiba Jobin-Yvon, Edison New Jersey, NJ) with an 1200 g/mm grating. Spectra were collected with a 1024 × 1024 pixel TE-cooled CCD camera (Andor Technology, model DV435, South Windsor, CT). The spectrometer allowed light reflected from different positions on the sensor surface being collected separately, therefore allowing both the analytic and reference channels to be probed simultaneously on the same sensor. Each channel consisted of a strip 20 mm L × 4 mm W of the MIH coated sensor, though the spot size probed spectroscopically consisted of a 4 mm × 4 mm area in the center of each channel. The SPR shift measured corresponds to the response of the MIH coating to chemical stimuli over the 16 mm^2 area.

2.2. MIH preparation

Two different self-assembled monolayers, formed from dithiobis(succinimidyl propionate) (DSP) and N-hydroxysuccinimide ester of 16-mercaptohexadecanoic acid (NHS-MHA) respectively, were evaluated for attachment of the MIH to sensor surfaces. DSP was purchased from Soltec Ventures, Inc. (Beverly, MA), whereas NHS-MHA was synthesized in-house following a previously described procedure [52].

DSP self-assembled monolayers were prepared by soaking freshly sputtered gold surfaces in 0.001 M DSP in dimethylsulfoxide (DMSO, MP Biomedicals, Solon, OH). Similarly, for the NHS-MHA self-assembled monolayer preparation, sensor surfaces were exposed to 0.005 M NHS-MHA in tetrahydrofuran (THF, Fisher Scientific, Fair Lawn, NJ). Modified gold surfaces were rinsed with DMSO or THF (depending of the SAM used), and then with water before being immediately used in the MIH preparation process.

The MIH synthesis employed in this study was modified from Parmpi and Kofinas [53] to yield membranes suitable for SPR analysis. Specifically, a 20 mL aqueous solution containing 0.1 mg/mL aqueous poly(allylamine hydrochloride) (PAH, Sigma–Aldrich, St. Louis, MO), 0.5 mg/mL D-glucose phosphate barium salt (GPS-Ba, Sigma–Aldrich, St. Louis, MO) and sufficient 1 M NaOH (Mallinckrodt, Paris, KY) to raise the solution pH to 9 (in order to partially neutralize the amine sites, rendering them available for subsequent tethering to the gold surface) was stirred for 30 min prior to addition of DSP-modified gold-coated slides. The 30 min delay allows for interaction and re-arrangement of the PAH around the template, initiating the formation of the analyte-recognizing cavities [53,54]. After 3 h, 5 mL of 0.03 M epichlorohydrin (Acros Organics, Morris Plains, NJ) were added to crosslink the hydrogel and the solution was stirred overnight. The slides were then removed from the solution, rinsed with deionized water and dipped in 4 M NaOH solution overnight to extract the template. Finally, sensors were dipped in stirred deionized water for 30 min to thoroughly rinse off the NaOH. Sensor slides with NHS-MHA were prepared similarly, except that 1 mg/mL GPS-Ba was added to the polymer solution and that 0.2 M NaOH was used to remove the template after imprinting. Finally the slides were dried under a stream of dry nitrogen (Keen Compressed Gas, Wilmington, DE) and stored under atmospheric conditions until used. For FT-IR studies, sensor slides were sputtered with 5 nm chromium followed by 150 nm of gold and prepared as described above. Mid-infrared absorption spectra were acquired with a Vertex 70 FT-IR spectrometer (Bruker Optics, Billerica, MA) equipped with a liquid nitrogen-cooled mercury–cadmium–telluride detector (Infrared Associates, Inc., Stuart, FL) at a 2 cm^{-1} resolution. Each spectrum represents an average of 100 scans. An AutoSeagull specular reflectance accessory (Harrick Scientific, Pleasantville, NY) permitted spectral collection at an incident angle of 87°. In order to minimize atmospheric contributions, the sample compartment of the FT-IR spectrometer was aggressively purged with dry nitrogen gas. Scanning electron micrographs were acquired using a XL-30 scanning electron microscope (FEI, Hillsboro, OR) equipped with a field emission electron gun and operating in environmental mode.

2.3. Gold nanoparticle preparation

Gold nanoparticles were synthesized by a modified Turkevitch method [55]. Initially, the pH of a 10 mL 0.001 M $HAuCl_4$ $3H_2O$ (Acros Organics, Morris Plains, NJ) solution was adjusted to 7.2 with 1 M NaOH. The solution was heated to boiling and 5% (w/w) sodium citrate (Fisher Scientific, Fair Lawn, NJ) was added to achieve a 2:1 ratio between citrate and $AuCl_4^-$. The boiling solution was continuously stirred for 1 h turning a wine-red color. The colloid solution was allowed to cool to room temperature at which point several drops of a 1 M cysteamine hydrochloride (Sigma–Aldrich, St. Louis, MO) in 1 M NaOH solution was added until the colloid solution turned blue, indicating that the gold nanoparticles were modified with the cysteamine capping agent. A 5 mL aliquot of this solution was added to the PAH solution immediately prior to the addition of epichlorohydrin. When gold nanoparticles were used the volume of 0.03 M epichlorohydrin was also adjusted to 6.25 mL to maintain the concentration of cross-linker. Characterization of the synthesized nanoparticles was performed with a JEM-2000fx transmission electron microscope (JEOL, Tokyo, Japan) equipped with a lanthanum hexaboride electron gun using an acceleration voltage of 200 kV. An aliquot of the freshly synthesized colloid solution was drop-casted onto 200-mesh carbon-coated nickel grids purchased from SPI Supplies (West Chester, PA). Size distribution was determined with the DigitalMicrograph software from Gatan Inc. (Pleasanton, CA).

2.4. Sugar detection in aqueous media

For SPR measurements, a custom-made dual channel poly(methyl methacrylate) flow-cell was used to divide the sensor surface into two separate sensing regions and to guide flow of solutions across the sensor surface. One channel was presented with the analyte in solution, while the other served as a reference channel to account for signal drifting from pressure changes, temperature fluctuation or other external factors. The sensor was fixed to the flow-cell with a gasket made from laboratory paraffin film (Parafilm, Pechiney Plastic Packaging, Menasha, WI). The liquid flowing system consisted of a Rainin Dynamax peristaltic pump model RP-1 (Rainin Instrument, LLC, Oakland, CA) and a series of valves connected by 1/16 in. polytetrafluoroethylene tubing and controlled by a custom-written LabView virtual instrument (National Instruments, Austin, TX). Experimental runs began with the collection of s-polarized reflectance spectra used to normalize the light output from the source. Rotating the linear polarizer 90° the p-polarized component required for plasmonic coupling. The SPR dip minima was located using automated 'minimum-hunting' MATLAB (Mathworks, Natick, MA) routines based on polynomial fitting of the parabolic SPR dip, with the roots of the fit corresponding to λ_{SPR}.

Each sensing cycle began with equilibration of the coating in water, followed by exposure to the analyte and then a water washing step to remove non-specifically bound species. At the end of each cycle, 0.1 M NaOH was flushed to regenerate the sensor surface. Each step lasted 10 min. The MIHs were evaluated for rebinding affinity towards glucose and structurally related sugars, fructose and sucrose, at various concentrations. Glucose, fructose and sucrose were all obtained from Sigma–Aldrich (St. Louis, MO).

2.5. Glucose detection in human urine

Urine sample collected from a healthy (non-diabetic) human male was used to verify the performance of the sensor exposed to physiological fluids. Prior to analysis, the urine was centrifuged to remove any particulate matter and the supernatant was spiked with 0.5–5.0 mg/mL glucose. Ammonium phosphate (Fisher Scientific, Fair Lawn, NJ), urea, uric acid and creatinine (all from Sigma–Aldrich, St. Louis, MO) at physiologically relevant concentrations [56] were dissolved in deionized water and used to condition the sensor prior to the SPR measurements. The collection conditions were identical to measurements performed with deionized water.

3. Results and discussion

3.1. MIH synthesis and characterization

Two SAMs with different carbon-chain lengths (C_3 versus C_{16}) were tested for MIH attachment to the gold SPR surfaces with no discernible difference in coating quality. This is not surprising since in the application described herein, the SAM is utilized merely as a tether site for the MIH, therefore, the length of the carbon chain is inconsequential.

Two contrasting processes are responsible for the formation of MIH coatings: the first one involves the availability of primary amines in neutralized PAH for reaction via amide coupling with the succinimidyl end-groups of the immobilized SAM and subsequent cross-linking upon addition of epichlorohydrin. The second process relies on the remaining amine salts in PAH to associate with the negatively charged phosphate groups of the template, forming the analyte binding sites in the MIH. Hence, control of the ratio between protonated and unprotonated amine groups present in solution is necessary, since attachment and cross-linking of the hydrogel network as well as the imprinting process itself are affected.

These processes were monitored by FT-IR spectroscopy; Fig. 1(A–C) displays graphically the influence of the relative concentration of protonated to unprotonated amine (as a function of pH) on the attachment of the hydrogel to SAM-modified gold surfaces, while Fig. 1(D–E) highlights the imprinting process of the hydrogel.

PAH binding to SAM-modified surfaces can be monitored as a function of the decreasing –C═O stretching peak absorbance at 1740 cm^{-1} associated with the NHS end-group. Concomitantly, the increasing symmetric and antisymmetric $–NH_2$ bands between 1500 and 1700 cm^{-1} further confirms attachment of the hydrogel to the surface [57]. At a pH value of 4 (see Fig. 1(A)) the –C═O peak was still prominent after a reaction time of 420 min, whereas it slowly decreases in intensity over 180 min at pH 9 (Fig. 1(B)) and completely disappears within 30 min at pH 11 (Fig. 1(C)). Comparison of the spectral time-series collected at the three pH values indicate that the rate of reaction between PAH and SAM concomitantly with the pH. The increase in intensity of the $–NH_2$ band confirms that amide coupling is favored at higher pHs. Estimation of the fraction of unprotonated amine groups in PAH ($pK_a \sim 9$ [58,59]), yields that at pH values of 4, 9 and 11 the primary amines represent approximately 0.001%, 50% and 99%, respectively, of the total amines present in the hydrogel. Since unprotonated amines are responsible for reaction with the NHS leaving group and covalently bind to the SAM, the pH influences the binding rate of the hydrogel to sensor surfaces. Hydrogel attachment at pH 4 (Fig. 1(A)) was not observed to occur to any appreciable extend, hence further studies focused exclusively on MIHs bound at pH values of 9 and 11.

Imprinting with the template was also evaluated by FT-IR spectroscopy. Using GPS-Ba as the template, instead of glucose, results in the formation of stronger GPS-Ba–hydrogel complex due to the ionic interaction. Because the MIH preparation is carried out in an aqueous environment, hydrogen bonding between glucose and amines cannot be relied on as the sole driving force for the imprinting process due to the interference of water [60,61]. Imprinting of the hydrogel with GPS-Ba yields an absorbance band

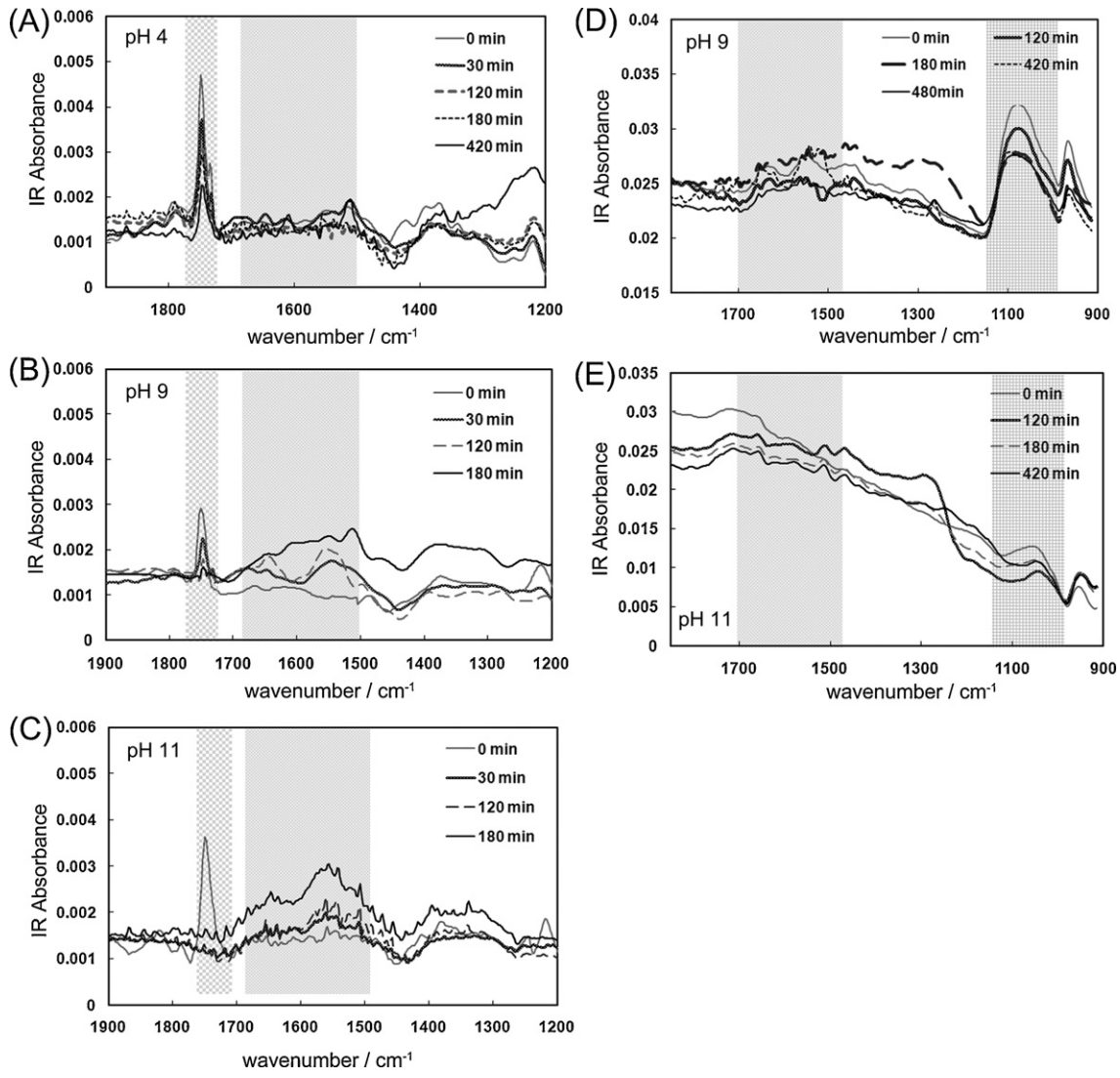

Fig. 1. The attachment of polymer via the NHS-MHA linker under (A) pH 4, (B) pH 9 and (C) pH 11, and the imprinting of GPS-Ba into PAH at (D) pH 9 and (E) pH 11 tracked by mid-IR spectroscopy. Each series of overlaid spectra corresponds to one slide. For (A–C) spectra of slides coated with NHS-MHA were taken after the indicated time in 1 mg/mL polymer solution without template; for (D) and (E) spectra of slides imprinted and cross-linked were taken after the indicated time stirring in DI water. Absorption peaks of interest are highlighted by grey shadows.

at approximately 1050 cm^{-1} associated with –P═O stretching of the phosphate group [57], indicating the incorporation of the template within the hydrogel. The FT-IR spectra in Fig. 1(D) indicate that at pH 9, where approximately half of the amine groups are protonated, a strong association between the phosphate group and the PAH is achieved, as demonstrated by retention of the phosphate group within the hydrogel even after exposure to DI water for 6 h. At pH 11 (Fig. 1(E)), most of the amine groups are deprotonated, therefore the ionic interaction between the template and the hydrogel is not possible, resulting in a comparatively weak –P═O absorption peak. These results indicate that at pH 9 a good compromise is achieved between efficient hydrogel attachment to gold surfaces, while maintaining sufficient amine salts capable of interacting with the template. Hence, all hydrogel mixtures used for sensor studies presented below were adjusted to a pH 9.

In addition to PAH binding and extent of complex formation, the relative concentrations of the template, polymer and cross-linker require further tuning to yield a high SPR response. Different MIH synthesis parameters were evaluated with respect to the highest performance (i.e., $\Delta RI/\Delta C$[glucose]) by exposing the sensor to 10 mg/mL aqueous glucose solution. The results are summarized in Table 1.

Hydrogel coatings immobilized in the absence of GPS-Ba serve to establish a baseline 'control' response to non-selective diffusion of glucose through the hydrogel. Utilizing PAH concentrations below 1 mg/mL yielded non-reproducible batch-to-batch MIH

Table 1
Measured response to 10 mg/mL glucose in DI water for membranes prepared with different amounts of polymer, template and cross-linker.

Coating	PAH (mg/mL)	Epichlorohydrin (mg/mL)	GPS-Ba (mg/mL)	$\Delta\lambda_{SPR}$ (nm, $\mu \pm 1\sigma$)
1	1.0	0.2	0.0	0.15 ± 0.03
2	1.0	0.2	0.05	0.18 ± 0.05
3	1.0	0.2	0.5	0.28 ± 0.03
4	1.0	0.5	0.0	0.12 ± 0.04
5	1.0	0.5	0.05	0.14 ± 0.03
6	1.0	0.5	0.5	0.38 ± 0.05
7	1.0	1.0	0.5	0.35 ± 0.07
8	2.0	0.5	0.5	0.27 ± 0.05

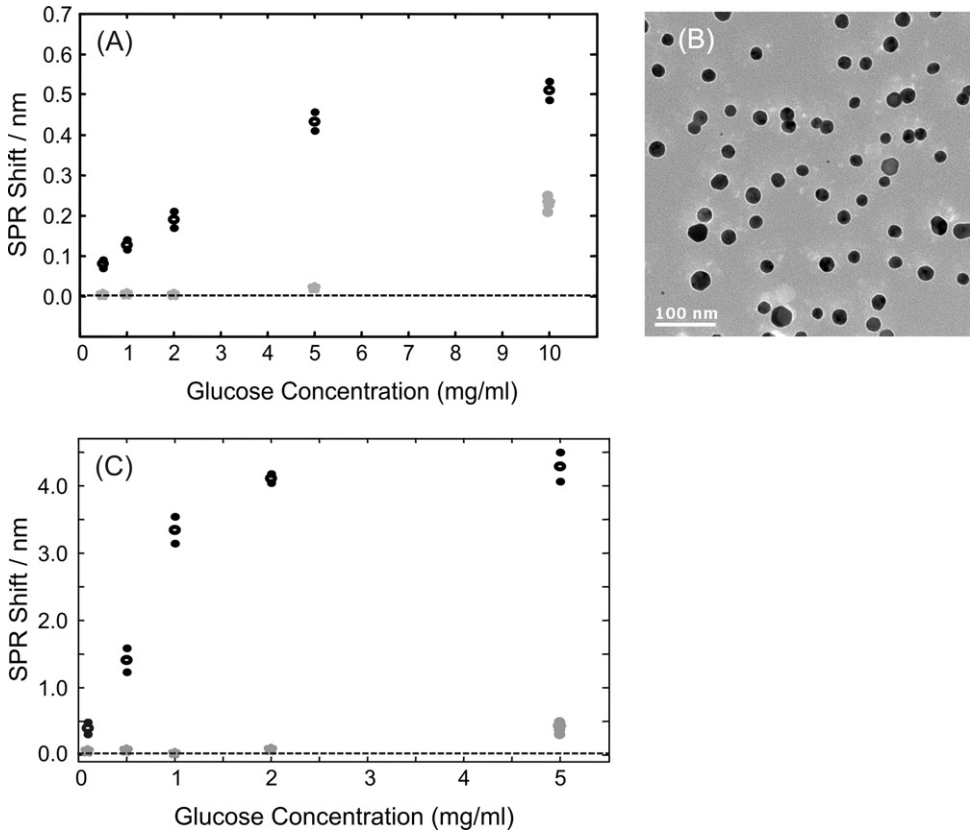

Fig. 2. (A) SPR response of imprinted (black circles) and non-imprinted (grey stars) hydrogel sensor to glucose in DI water. Results came from different slides and error bars stand for 95% confidence interval. Precision of SPR shift is shown by plus/minus standard deviation of the mean (black dots, usually $n = 3$). (B) A TEM image of gold nanoparticles used. (C) SPR response of imprinted (black circles) and non-imprinted (grey stars) hydrogel sensor embedded with gold nanoparticles to glucose in DI water. Results came from different slides and error bars stand for 95% confidence interval. Precision of SPR shift is shown by plus/minus standard deviation of the mean (black dots, usually $n = 3$).

membranes, therefore no data could be included in Table 1. In contrast, PAH concentrations approaching 2 mg/mL (coating 8) and higher produced broad SPR dips (i.e. SPR coupling occurring at multiple conditions) due to coating heterogeneity within the plasmonically probed volume. Since measuring the response to the analyte is contingent upon precisely locating (in terms of wavelength) the SPR dip minima, broader dips render this procedure challenging. Coatings labeled 1 and 4 both serve as non-imprinted hydrogel (NIH) controls illustrating that non-selective absorption from a 10 mg/mL glucose solution yields a λ_{SPR} shift of approximately 0.15 nm. Addition of 0.05 mg/mL GPS-Ba (coatings 2 and 5) did not improve the response to the analyte beyond levels already attributed to non-specific interactions. Raising the concentration of the template to 0.5 mg/mL (coatings 3 and 6) resulted in the formation of sufficient template binding cavities to yield a statistically relevant λ_{SPR} shift. Comparison of MIHs formed with increasing levels of cross-linker (coatings 3, 6 and 7) indicate that structural rigidity of the hydrogel will influence the performance measured. From three epichlorohydrin concentrations investigated, it is evident that "softer" hydrogels obtained at lower concentrations do not exhibit the same level of response to 10 mg/mL glucose as the two 'more rigid' counterparts. In part this may be due to the fact that a malleable carbon network is better capable of accommodating enriched analyte molecules within the free volume of the hydrogel, resulting in a lower degree of swelling. In contrast, a more rigid structure is forced to expand upon incorporation of the analyte since the carbon network in unable to re-adjust itself around the analyte.

Cross-linker concentration greater than 1 mg/mL were not pursued in this initial contribution because a structurally rigid coating, less amenable to swelling, and therefore displaying smaller λ_{SPR} shifts, is anticipated. For the binding studies presented herein, a cross-linker concentration of 0.5 mg/mL was used since it provided sufficient rigidity for selective cavities to retain their shape after template removal as well as enabling swelling of the MIH upon glucose re-binding.

3.2. Physical characterization

As was previously mentioned, RI changes monitored by SPR spectroscopy are non-selective. Therefore, discrimination of λ_{SPR} shift induced by bulk RI changes associated with solutions containing different glucose concentrations (e.g. a false positive) from λ_{SPR} shifts resulting from selective analyte uptake, is achieved by employing MIH membranes with thicknesses greater than penetration depth (d_p) of surface plasmons (approximately 200–300 nm [14]).

Scanning electron micrographs acquired along fractured edges provide an approach for evaluating MIH thickness. By this method, MIH thickness ranged from approximately 0.8 μm to 2.5 μm. Therefore, λ_{SPR} shifts recorded reflect refractive index changes within the MIH rather than in the bulk liquid. The micrograph also reveals superficial accumulations ranging from 1 μm to 5 μm in size atop the relatively uniform background. The origin of these features is still unknown though it is likely that they correspond

to hydrogel agglomerations formed in solution and bound to the coated sensor during later stages of MIH synthesis.

3.3. Glucose detection

Evaluation of MIH-coated sensors involved measuring glucose solutions with different concentrations. Sensor slides coated with MIH but without gold nanoparticles reached equilibrium response to the analyte within 2 min and displayed an increasing λ_{SPR} shift with glucose concentrations below ~5 mg/mL (Fig. 2(A)).

As was previously mentioned, control NIHs were prepared in exactly the same way as MIHs but without the template. In all measurements, the response obtained with NIH was lower compared to imprinted hydrogels. Furthermore, NIH sensors required glucose concentrations greater than 5 mg/mL in order to register measurable shifts in λ_{SPR}. The difference in response between MIH and NIH suggest the presence of selective binding sites in the imprinted hydrogel, as well as indicating that non-specific interactions, such as surficial adsorption and non-specific diffusion of glucose, do not contribute significantly to the SPR response measured.

3.4. Addition of gold nanoparticles

The interaction between metallic nanoparticles, especially gold nanoparticles, and freely propagating plasmons excited at continuous metal films has been previously described as a method for enhancing the SPR sensitivity [45–47,49–51,62]. In order to evaluate the influence of nanoparticles on MIHs, cysteamine-capped gold nanoparticles were embedded into the hydrogel by cross-linking the amine groups of the capping agent with unprotonated primary amines in PAH. An exemplary transmission electron microscopic image of the nanoparticles synthesized is shown in Fig. 2(B). A distribution study of the images recorded indicates that the gold nanoparticles have a diameter of 25 ± 8 nm.

The response of MIH-coated sensors containing gold nanoparticles to aqueous glucose solutions of different concentrations is summarized graphically in Fig. 2(C). Comparison with the results shown in Fig. 2(A) demonstrate that addition of gold nanoparticles produces a 10- to 15-fold improvement in the amplitude of the SPR signal as well as increased sensitivity at low glucose concentrations (<1 mg/mL). In contrast, control experiments with NIH membranes containing gold nanoparticles showed a comparatively small response to non-specific binding of glucose. The linear range of gold nanoparticles-MIH sensors decreased compared to MIH sensors without nanoparticles, as well as reaching saturation levels at lower glucose concentrations: 5 mg/mL versus 10 mg/mL for coatings with and without gold nanoparticles, respectively. A possible explanation for these observations is that the number of binding sites available inside the sensing layer is altered considerably by the incorporation of the nanoparticles. It may also be more difficult for glucose molecules to diffuse into the sensing layer during measurement when the layer is embedded with nanoparticles. Indeed comparison of the response of MIH and Au-MIH membranes to glucose shows that the presence of gold nanoparticles delays the onset of a stable response, as depicted in the sensorgrams shown in Fig. 3.

The working concentration range of gold nanoparticles-MIH membranes cover the critical glucose concentrations in plasma tests [63,64] and urine glucose screening [65,66] for diagnosis of diabetes, and its upper limit is comparable to typical non-enzymatic glucose sensors reported [67–71]. From calibration, the limit of detection of the gold nanoparticle-MIH sensor in water was determined to be 0.02 mg/mL (S/N = 3 based on standard deviation of the MIH response in a blank solution) and a limit of quantification of 0.06 mg/mL (based on 10 standard deviations of the MIH response in a blank solution) and a sensitivity of 1.9 nm (mg/mL glucose)$^{-1}$ in deionized water.

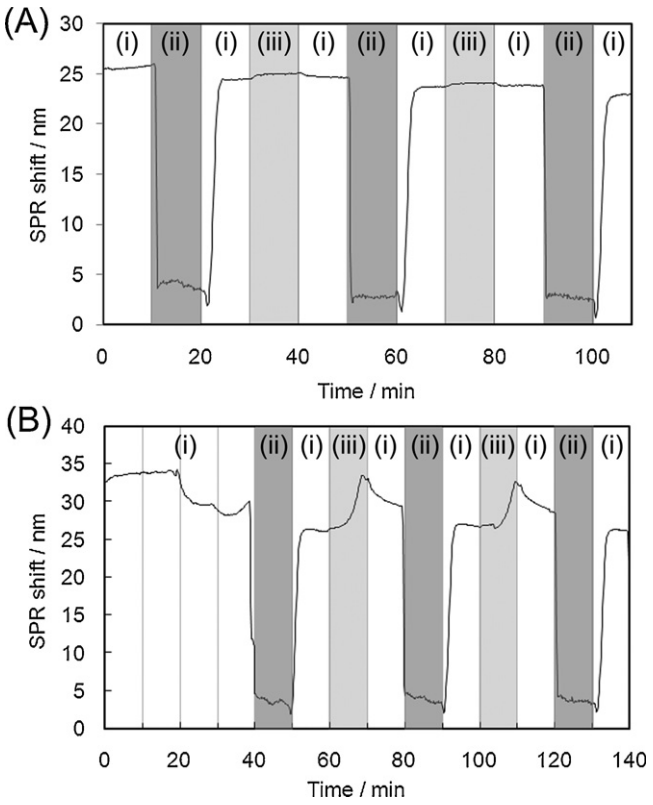

Fig. 3. Exemplary sensorgrams of (A) MIH and (B) Au-MIH coated sensor detecting 1 mg/mL glucose in water. The sensor was rinsed with (i) deionized water, (ii) 0.1 M NaOH and (iii) 1 mg/mL.

Upon glucose binding and MIH swelling, a red-shift in the resonant wavelength was observed, which is in sharp contrast to the blue-shift expected from the increased distance between the gold nanoparticles and the underlying gold film (so-called "gap-mode" [48,49,72]). SPR responses are enhanced by plasmonic coupling if the distance, d, between the two plasmon active entities is maintained within the radius of the nanoparticle or smaller [73]. For the nanoparticles utilized herein, $r \sim 13$ nm. Considering that the MIH synthesis was carried out by mixing all components in one vessel, it is likely that the nanoparticles are randomly distributed within the 0.8 μm thick membrane, and that most of them reside at $d > 13$ nm. Therefore, the 10-fold increase in measured signal most likely rises from the increased bulk RI of the composite gold nanoparticles-MIH membrane.

It is worth noting that the comparatively large error bars (on average approx. ±0.15 nm) reported in Fig. 2(C) result from measurements taken with different sensors, providing an estimate of batch-to-batch variability as opposed to variability within the same sensor. Glucose response was observed to decrease during repeated cycles, though this is possibly associated with degradation of the coating by the 0.1 M NaOH washing step used to release the analyte and regenerate the MIH. Finally, Fig. 2(A and C) suggest a Langmuir adsorption behavior. Though at first glance it may appear to appropriately describe the MIH response to glucose, modeling of adsorption processes at imprinted matrices is complicated by the failure to satisfy two of the basic requirements: monolayer adsorption and binding sites homogeneity. The lack of consensus regarding a 'correct' isotherm used for imprinted matrices has resulted in a variety of models being invoked to explain the binding event [74–76]. Therefore, at this stage, modeling of glucose re-binding was deferred.

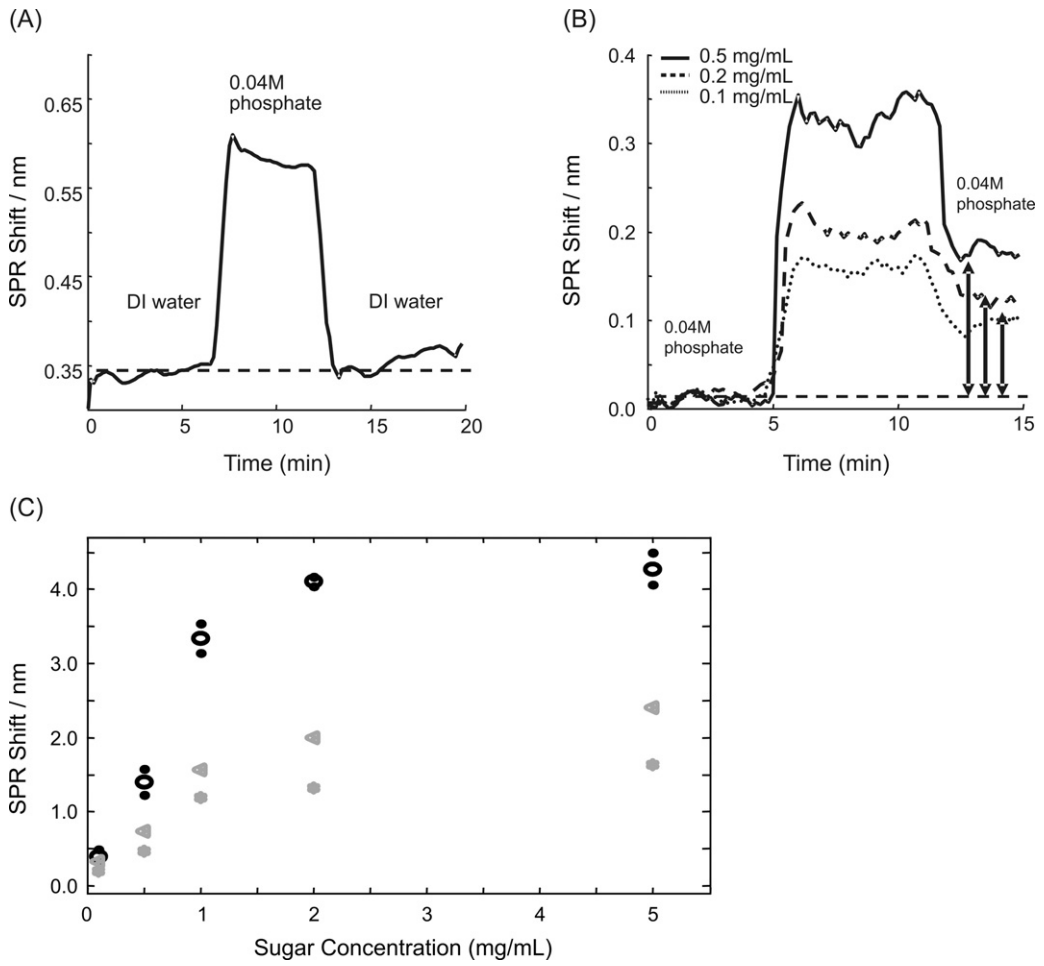

Fig. 4. Sensor performances in presence of interferences. (A) SPR response of MIH sensor to 60 mM aqueous phosphate only. (B) SPR response of MIH sensor to glucose added to 40 mM aqueous phosphate solution in different concentrations (0.1, 0.2 and 0.5 mg/ml). (C) SPR response of Au-MIH sensor to glucose (black circles), fructose (grey triangles) and sucrose (grey stars). Results were obtained from different MIH coatings. Precision of SPR shift is shown by plus/minus standard deviation of the mean (black dots, usually $n = 3$ for glucose samples). Individual sucrose and fructose samples were not replicated.

3.5. Interference studies

The formation of recognition sites for glucose in the sensing hydrogel is facilitated by ionic bonding of protonated amines in PAH with phosphate groups in GPS-Ba. Since a significant amount of phosphate (0.03–0.06 M) is present in urine [56] it is necessary to evaluate whether the presence of phosphate groups can interfere with the MIH ability to bind to glucose. Initial studies involving MIH coatings exposed to intermittent phosphate plumes did not show a net λ_{SPR} shift (i.e., the signal returned to baseline levels immediately upon flushing with deionized water) indicating that phosphate groups do not permanently re-bind to available amines in PAH (Fig. 4(A)). Spiking 0.06 M ammonium phosphate solutions with the analyte showed a response similar in magnitude to the SPR response of glucose in DI water suggesting that physiologically relevant levels of phosphate in urine are unlikely to interfere. Exemplary sensorgrams are depicted in Fig. 4(B), which show a net λ_{SPR} shift due to glucose re-binding.

Another source of potential interferents for imprinted matrices rises from cross-reactivity with structurally related compounds. Hence, selective glucose recognition was examined by exposing the gold nanoparticles-MIH coatings to similar sugars. Fig. 4(C) summarizes the λ_{SPR} shift measured with fructose and sucrose solutions. Fructose is structurally related to glucose, yet induces a significantly smaller response suggesting that although fructose is capable of binding to some of the recognition sites, the MIH preferentially binds to the template. The response measured with sucrose is even smaller than that for fructose. Sucrose is larger than either glucose or fructose, therefore, it can be anticipated that hindered diffusion through the MIH will affected the response level in addition to size incompatibility with most of the recognition sites.

Cross-reactivity between molecularly imprinted materials and compounds structurally related to the template is common and can be minimized by careful choice of synthetic parameters (e.g. solvent, starting monomers) [74,77]; with regards to glucose monitoring, fructose has been previously recognized as a potential interferent [32,53,78]. This presents a challenge for sensing platforms aimed at single-compound detection in complex media. An approach to mitigate cross-reactivity with molecularly imprinted materials involves the use of sensor arrays, wherein coatings with different specificities (analyte and interferents) are utilized and the response obtained is mathematically treated to deconvolute the analytic from the interfering signal [79].

In addition to phosphate, urine also contains a number of molecular species with amine groups (urea, uric acid and creatinine). To test their effect on the MIH coatings, a mixture of these compounds at concentrations commonly found in urine [56] was prepared and

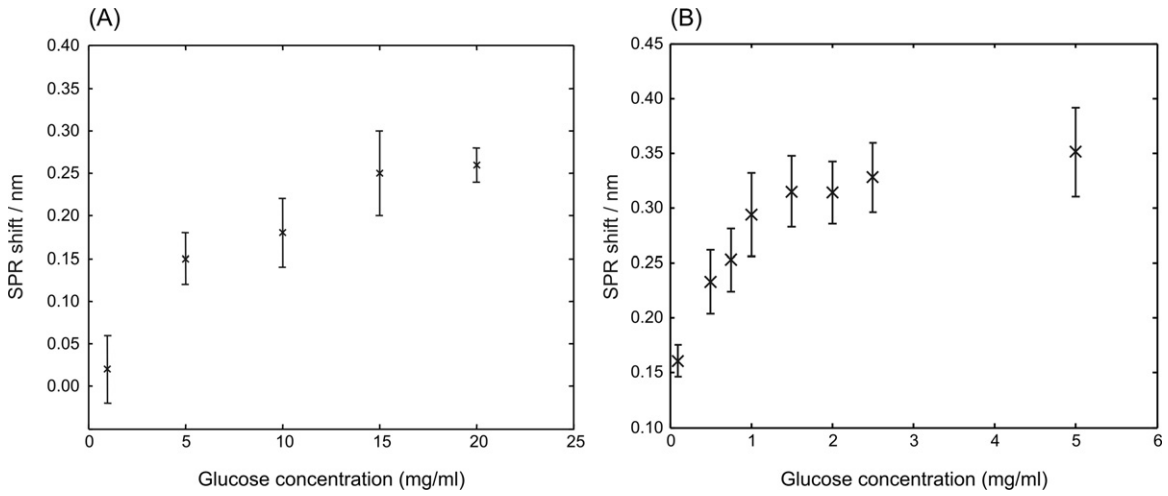

Fig. 5. Response of (A) MIH and (B) Au-MIH coated glucose sensor in undiluted urine spiked with different concentration of glucose.

presented to the sensor similarly to the phosphate experiments described above (except for replacing titrated phosphate solution with the mixture), and it was indicated by the results that these compounds showed no net affect either.

Finally, glucose detection in human urine was explored. The matrix resulted from combining multiple urine collections from a healthy, non-diabetic individual throughout one day, homogenizing any temporal variations in composition. The matrix was centrifuged to remove potential sediment and spiked with glucose at different amount. Fig. 5 shows the response of MIH coatings without and with gold nanoparticle to the spike urine. The measured response decreased significantly compared to sample solutions prepared with DI water. The limit of detection and limit of quantification for urine analysis with Au-MIH were determined to be 0.12 mg/mL and 0.40 mg/mL, respectively, with a sensitivity of approximately 0.34 nm (mg/mL glucose)$^{-1}$. There are three possible contributing factors, all acting to decrease the MIH sensitivity to glucose. PAA hydrogels undergo contraction when exposed to salt solutions due to increased osmotic pressure [80]. Therefore, it is possible that MIH coatings in urine are prevented from swelling when incorporating glucose to the same extent as in DI water. Similarly, it is likely that some of the binding cavities distort and collapse rending them incapable of interacting with the analyte. Additionally, to the extent that hydrogen bonding between glucose and the amine functional groups in the MIH influence sensitivity, increasing ionic strength decreases the amount of intermolecular hydrogen bonding [81].

The limit of detection for the Au-MIH membranes (0.12 mg/mL) is within levels anticipated for glucose content in the urine of healthy individuals (0.06–0.15 mg/mL [78,82–84]) and is comparable to other recent reports [85–89]. The decreased dynamic range, however, renders quantification of glucose at elevated levels difficult. Considering that glucose levels can spike to over 6 mg/mL [85] shortly after ingesting a meal and the sensor's inability to differentiate between glucose concentrations above ~1 mg/mL, this first iteration the sensor would only reliably function for threshold sensing, discriminating between glucose levels in healthy or diabetic individuals. If needed, samples could be diluted to expand the dynamic range to higher concentrations. Done in an automated manner this would not significantly increase the variance of analyses at the expense of a greater dynamic range. Regardless, despite the current lack of sensitivity necessary for precise monitoring in urine, these results provide a first approximation of the achievable detection limits as well as highlighting some of the challenges rising from performing measurements in complex solutions.

4. Conclusion

A SPR sensing system with hydrophilic molecularly imprinted hydrogel as recognition unit was developed for glucose monitoring. Swelling of the hydrogel sensing layer due to combination with glucose was tracked by SPR spectroscopy. While further refinements are necessary to improve sensitivity of the chemical recognition layer, the system displays potential as a specific detection method for glucose monitoring in a complex physiological fluid. Cooperation of gold nanoparticles has significantly enhanced the sensor's response and sensitivity at low glucose concentrations. The sensor showed selective response to glucose compared to fructose and sucrose, and was capable to detect glucose spiked in deionized water at the μg/mL level. Preliminary analysis of glucose in urine indicates that high ionic strength media may be disrupting the re-binding event, decreasing the MIH sensitivity.

Acknowledgements

The authors would like to thank Delaware's EPSCoR program (grant no. DIBO312214) and the American Heart Association (N.M, grant no. 09POST2120014) for partial funding. W.P. acknowledges the National Natural Science Foundation of China for partial support (grant no. 60977055/61137005).

References

[1] G. Giraudi, L. Anfossi, I. Rosso, C. Baggiani, C. Giovannoli, C. Tozzi, Anal. Chem. 71 (20) (1999) 4697–4700.
[2] K.D. Altria, D. Elder, J. Chromatogr. A 1023 (1) (2004) 1–14.
[3] A.K. Su, J.T. Liu, C.H. Lin, Talanta 67 (4) (2005) 718–724.
[4] B.R. Baker, R.Y. Lai, M.S. Wood, E.H. Doctor, A.J. Heeger, K.W. Plaxco, J. Am. Chem. Soc. 128 (10) (2006) 3138–3139.
[5] D.C. Grant, R.J. Helleur, Anal. Bioanal. Chem. 391 (8) (2008) 2811–2818.
[6] Y. Fintschenko, A.J. Krynitsky, J.W. Wong, J. Agric. Food Chem. 58 (10) (2010) 5859–5861.
[7] A. Vonaparti, E. Lyris, Y.S. Angelis, I. Panderi, M. Koupparis, A. Tsantili-Kakoulidou, R.J.B. Peters, M.W.F. Nielen, C. Georgakopoulos, Rapid Commun. Mass Spectrom. 24 (11) (2010) 1595–1609.
[8] S. Banerji, W. Peng, Y.C. Kim, N. Menegazzo, K.S. Booksh, Sens. Actuators B: Chem. 147 (1) (2010) 255–262.
[9] S.W. Choi, H.J. Chang, N. Lee, J.H. Kim, H.S. Chun, J. Agric. Food Chem. 57 (4) (2009) 1113–1118.
[10] H.V. Hsieh, Z.A. Pfeiffer, T.J. Amiss, D.B. Sherman, J.B. Pitner, Biosens. Bioelectron. 19 (7) (2004) 653–660.
[11] E. Mauriz, A. Calle, A. Abad, A. Montoya, A. Hildebrandt, D. Barcelo, L.M. Lechuga, Biosens. Bioelectron. 21 (11) (2006) 2129–2136.
[12] E. Mauriz, A. Calle, L.M. Lechuga, J. Quintana, A. Montoya, J.J. Manclus, Anal. Chim. Acta 561 (1–2) (2006) 40–47.

[13] E. Mauriz, A. Calle, J.J. Manclus, A. Montoya, A.M. Escuela, J.R. Sendra, L.M. Lechuga, Sens. Actuators B: Chem. 118 (1–2) (2006) 399–407.
[14] R.B.M. Schasfoort, A.J. Tudos, Handbook of Surface Plasmon Resonance, Royal Society of Chemistry, Cambridge, 2008.
[15] J. Homola, Chem. Rev. 108 (2) (2008) 462–493.
[16] R.J. Green, R.A. Frazier, K.M. Shakesheff, M.C. Davies, C.J. Roberts, S.J.B. Tendler, Biomaterials 21 (18) (2000) 1823–1835.
[17] J.F. Masson, T.M. Battaglia, P. Khairallah, S. Beaudoin, K.S. Booksh, Anal. Chem. 79 (2) (2007) 612–619.
[18] X.D. Fan, I.M. White, S.I. Shopoua, H.Y. Zhu, J.D. Suter, Y.Z. Sun, Anal. Chim. Acta 620 (1–2) (2008) 8–26.
[19] J. Mitchell, Sensors 10 (8) (2010) 7323–7346.
[20] J. Homola, Surface Plasmon Resonance Based Sensors, Springer, Berlin, 2006.
[21] R. Gupta, A. Kumar, Biotechnol. Adv. 26 (6) (2008) 533–547.
[22] R. Shoji, T. Takeuchi, I. Kubo, Anal. Chem. 75 (18) (2003) 4882–4886.
[23] K. Sode, S. Ohta, Y. Yanai, T. Yamazaki, Biosens. Bioelectron. 18 (12) (2003) 1485–1490.
[24] A. Ersoz, A. Denizli, A. Ozcan, R. Say, Biosens. Bioelectron. 20 (11) (2005) 2197–2202.
[25] M. Javanbakht, S.E. Fard, A. Mohammadi, M. Abdouss, M.R. Ganjali, P. Norouzi, L. Safaraliee, Anal. Chim. Acta 612 (1) (2008) 65–74.
[26] A. Kugimiya, T. Takeuchi, Biosens. Bioelectron. 16 (9–12) (2001) 1059–1062.
[27] O.A. Raitman, V.I. Chegel, A.B. Kharitonov, M. Zayats, E. Katz, I. Willner, Anal. Chim. Acta 504 (1) (2004) 101–111.
[28] R.B. Pernites, R.R. Ponnapati, R.C. Advincula, Macromolecules 43 (23) (2010) 9724–9735.
[29] A. Heller, B. Feldman, Chem. Rev. 108 (7) (2008) 2482–2505.
[30] N.S. Oliver, C. Toumazou, A.E.G. Cass, D.G. Johnston, Diabet. Med. 26 (3) (2009) 197–210.
[31] K.E. Toghill, R.G. Compton, Int. J. Electrochem. Sci. 5 (9) (2010) 1246–1301.
[32] Y. Yoshimi, A. Narimatsu, K. Nakayama, S. Sekine, K. Hattori, K. Sakai, J. Artif. Organs 12 (4) (2009) 264–270.
[33] D. Rathod, C. Dickinson, D. Egan, E. Dempsey, Sens. Actuator B: Chem. 143 (2) (2010) 547–554.
[34] D. Feng, F. Wang, Z.L. Chen, Sens. Actuator B: Chem. 138 (2) (2009) 539–544.
[35] A.S. Hoffman, Adv. Drug Deliv. Rev. 54 (1) (2002) 3–12.
[36] G. Gerlach, K.-F. Arndt (Eds.), Hydrogel Sensors And Actuators, Springer-Verlag, Berlin, 2009.
[37] M.-S. Steiner, A. Duerkop, O.S. Wolfbeis, Chem. Soc. Rev. Adv. Article (2011).
[38] A. Molinelli, J. O'Mahony, K. Nolan, M.R. Smyth, M. Jakusch, B. Mizaikoff, Anal. Chem. 77 (16) (2005) 5196–5204.
[39] J. O'Mahony, A. Molinelli, K. Nolan, M.R. Smyth, B. Mizaikoff, Biosens. Bioelectron. 20 (9) (2005) 1884–1893.
[40] J. O'Mahony, A. Molinelli, K. Nolan, M.R. Smyth, B. Mizaikoff, Biosens. Bioelectron. 21 (7) (2006) 1383–1392.
[41] J. Wang, H.S. Zhou, Anal. Chem. 80 (18) (2008) 7174–7178.
[42] J. Mitchell, Sensors 10 (2010) 7323–7346.
[43] A. Baba, P. Taranekar, R.R. Ponnapati, W. Knoll, R.C. Advincula, ACS Appl. Mater. Interfaces 2 (8) (2010) 2347–2354.
[44] S. Banerji, W. Peng, Y.-C. Kim, N. Menegazzo, K.S. Booksh, Sens. Actuators B B147 (1) (2010) 255–262.
[45] J. Matsui, M. Takayose, K. Akamatsu, H. Nawafune, K. Tamaki, N. Sugimoto, Analyst 134 (1) (2009) 80–86.
[46] L.A. Lyon, M.D. Musick, M.J. Natan, Anal. Chem. 70 (24) (1998) 5177–5183.
[47] L.A. Lyon, W.D. Holliway, M.J. Natan, Rev. Sci. Instrum. 70 (4) (1999) 2076–2081.
[48] I. Tokareva, I. Tokarev, S. Minko, E. Hutter, J.H. Fendler, Chem. Commun. (31) (2006) 3343–3345.
[49] J. Matsui, K. Akamatsu, S. Nishiguchi, D. Miyoshi, H. Nawafune, K. Tamaki, N. Sugimoto, Anal. Chem. 76 (5) (2004) 1310–1315.
[50] S. Chah, E. Hutter, D. Roy, J.H. Fendler, J. Yi, Chem. Phys. 272 (1) (2001) 127–136.
[51] J. Matsui, K. Akamatsu, N. Hara, D. Miyoshi, H. Nawafune, K. Tamaki, N. Sugimoto, Anal. Chem. 77 (13) (2005) 4282–4285.
[52] T.M. Battaglia, J.F. Masson, M.R. Sierks, S.P. Beaudoin, J. Rogers, K.N. Foster, G.A. Holloway, K.S. Booksh, Anal. Chem. 77 (21) (2005) 7016–7023.
[53] P. Parmpi, P. Kofinas, Biomaterials 25 (10) (2004) 1969–1973.
[54] X. Feas, L. Ye, S.V. Hosseini, C.A. Fente, A. Cepeda, Polym. Int. 59 (1) (2010) 11–15.
[55] X.H. Ji, X.N. Song, J. Li, Y.B. Bai, W.S. Yang, X.G. Peng, J. Am. Chem. Soc. 129 (45) (2007) 13939–13948.
[56] D.F. Putnam, Composition and Concentrative Properties of Human Urine, Adv. Biotechnol. Power Dep., McDonnell Douglas Astronaut. Co, Huntington Beach, CA, USA, 1971, p. 107.
[57] D. Lin-Vien, The Handbook of Infrared and Raman Characteristic Frequencies of Organic Molecules, Academic Press, Boston, 1991.
[58] K. Iio, N. Minoura, M. Nagura, Polymer 36 (13) (1995) 2579–2583.
[59] S. Kobayashi, M. Tokunoh, T. Saegusa, F. Mashio, Macromolecules 18 (12) (1985) 2357–2361.
[60] C. Aleman, J.J. Navas, S. Munozguerra, J. Phys. Chem. 99 (49) (1995) 17653–17661.
[61] C. Aleman, M.C. Vega, L. Tabernero, J. Bella, J. Phys. Chem. 100 (27) (1996) 11480–11487.
[62] L. He, M.D. Musick, S.R. Nicewarner, F.G. Salinas, S.J. Benkovic, M.J. Natan, C.D. Keating, J. Am. Chem. Soc. 122 (38) (2000) 9071–9077.
[63] B. Zinman, J. Gerich, J.B. Buse, A. Lewin, S. Schwartz, P. Raskin, P.M. Hale, M. Zdravkovic, L. Blonde, Diabetes Care 33 (3) (2010) 692.
[64] T. Kuzuya, S. Nakagawa, J. Satoh, Y. Kanazawa, Y. Iwamoto, M. Kobayashi, K. Nanjo, A. Sasaki, Y. Seino, C. Ito, K. Shima, K. Nonaka, T. Kadowaki, Diabetes Res. Clin. Pract. 55 (1) (2002) 65–85.
[65] T. Urakami, S. Kubota, Y. Nitadori, K. Harada, M. Owada, T. Kitagawa, Diabetes Care 28 (8) (2005) 1876–1881.
[66] J.K. Davidson, Clinical Diabetes Mellitus: A Problem-Oriented Approach, Thieme, New York, 2000.
[67] F. Xiao, F.Q. Zhao, D.P. Mei, Z.R. Mo, B.Z. Zeng, Biosens. Bioelectron. 24 (12) (2009) 3481–3486.
[68] Z.L. Cheng, E.K. Wang, X.R. Yang, Biosens. Bioelectron. 16 (3) (2001) 179–185.
[69] E. Shoji, M.S. Freund, J. Am. Chem. Soc. 124 (42) (2002) 12486–12493.
[70] Y. Li, Y.Y. Song, C. Yang, X.H. Xia, Electrochem. Commun. 9 (5) (2007) 981–988.
[71] O.S. Wolfbeis, M. Schaferling, A. Durkop, Microchim. Acta 143 (4) (2003) 221–227.
[72] R.T. Hill, J.J. Mock, Y. Urzhumov, D.S. Sebba, S.J. Oldenburg, S.-Y. Chen, A.A. Lazarides, A. Chilkoti, D.R. Smith, Nano Lett. 10 (10) (2010) 4150–4154.
[73] S.E. Kawata, Near-Field Optics and Surface Plasmon Polaritons, Springer-Verlag Berlin, 2001.
[74] B. Sellergren (Ed.), Molecularly Imprinted Polymers: Man-Made Mimics of Antibodies and their Applications in Analytical Chemistry, Elsevier Science, Amsterdam, 2001.
[75] R.J. Umpleby II, S.C. Baxter, Y. Chen, R.N. Shah, K.D. Shimizu, Anal. Chem. 73 (19) (2001) 4584–4591.
[76] X. Li, S.M. Husson, Biosens. Bioelectron. 22 (3) (2006) 336–348.
[77] M. Yan, R. Olof (Eds.), Molecularly Imprinted Materials: Science and Technology, CRC Press, New York, 2005.
[78] S. Manju, P.R. Hari, K. Sreenivasan, Biosens. Bioelectron. 26 (2) (2010) 894–897.
[79] K.D. Shimizu, C.J. Stephenson, Curr. Opin. Chem. Biol. 14 (6) (2010) 743–750.
[80] G.V.R. Rao, T. Konishi, N. Ise, Macromolecules 32 (22) (1999) 7582–7586.
[81] G. Qun, W. Ajun, Carbohydr. Polym. 64 (1) (2006) 29–36.
[82] M.C. Moreno-Bondi, O.S. Wolfbeis, M.J.P. Leiner, B.P.H. Schaffar, Anal. Chem. 62 (21) (1990) 2377–2380.
[83] J. Fine, Br. Med. J. 1965–1 (5444) (1965) 1209–1214.
[84] D.K. Sen, G.S. Sarin, Br. J. Ophthalmol. 64 (9) (1980) 693–695.
[85] M. Miyashita, N. Ito, S. Ikeda, T. Murayama, K. Oguma, J. Kimura, Biosens. Bioelectron. 24 (5) (2009) 1336–1340.
[86] F. Xiao, F. Zhao, D. Mei, Z. Mo, B. Zeng, Biosens. Bioelectron. 24 (12) (2009) 3481–3486.
[87] R. Irawan, Y.H. Cheng, W.M. Ng, M.M. Aung, I.K. Lao, V. Thaveeprungsriporn, Biosens. Bioelectron. 26 (2011) 3666–3669.
[88] Y. Liu, C. Deng, L. Tang, A. Qin, R. Hu, J.Z. Sun, B.Z. Tang, J. Am. Chem. Soc. 133 (4) (2011) 660–663.
[89] X. Gao, W. Yang, P. Pang, S. Liao, Q. Cai, K. Zeng, C.A. Grimes, Sens. Actuators B B128 (1) (2007) 161–167.